DMD Fast Forward. Published on January 25, 2012 as doi:10.1124/dmd.111.043828
This article has not been copyedited and formatted. The final version may differ from this version.

DMD #43828

The impact of SNPs on human Aldehyde Oxidase

Tobias Hartmann, Mineko Terao, Enrico Garattini, Christian Teutloff, Joshua F. Alfaro, Jeffrey P. Jones, and Silke Leimkühler

Department of Molecular Enzymology, Institute of Biochemistry and Biology, University of Potsdam, Karl-Liebknecht-Str. 24-25, 14476 Potsdam, Germany (T.H., S.L.);

Laboratory of Molecular Biology, Department of Biochemistry and Molecular Pharmacology, Istituto di Ricerche Farmacologiche Mario Negri, via La Masa 19, 20156 Milano, Italy (M.T., E.G.);

Institute for Experimentalphysics, Free University of Berlin, Arnimallee 14, 14195 Berlin, Germany (C.T.);

Department of Chemistry, Washington State University, Pullman, WA 99163, USA (J.F.A., J.P.J.).

DMD Fast Forward. Published on January 25, 2012 as DOI: 10.1124/dmd.111.043828
This article has not been copyedited and formatted. The final version may differ from this version.

Running Title: Characterization of single nucleotide polymorphisms of hAOX1

† *Corresponding author:*

Silke Leimkühler, Tel: +49-331-977-5603, Fax: +49-331-977-5128,

E-mail: sleim@uni-potsdam.de

Text Pages (including references): 27

Tables: 3

Figures: 5

References: 43

Abstract : 248

Introduction : 922

Discussion : 1623

Abbreviations: AOX1: aldehyde oxidase 1; AO: aldehyde oxidase; XOR: xanthine oxidoreductase; XO: xanthine oxidase; XDH: xanthine dehydrogenase; Moco: molybdopterin cofactor; MCSF: moco sulfurase; DTT: dithiothreitol.

DMD Fast Forward. Published on January 25, 2012 as DOI: 10.1124/dmd.111.043828
This article has not been copyedited and formatted. The final version may differ from this version.

Abstract

Aldehyde oxidase (AO) is a complex molybdoflavoprotein that belongs to the xanthine oxidase family. AO is active as a homodimer and each 150 kDa monomer binds two distinct [2Fe2S] clusters, FAD and the molybdenum cofactor (Moco). AO has an important role in the metabolism of drugs based on its broad substrate specificity oxidizing aromatic aza-heterocycles, e.g. N^1-methylnicotinamide and N-methylphthalazinium, or aldehydes, such as benzaldehyde, retinal and vanillin. Sequencing of the 35 coding exons of the human *AOX1* gene in a sample of 180 Italian individuals led to the identification of relatively frequent synonymous, missense and nonsense single nucleotide polymorphisms (SNPs). Human aldehyde oxidase (hAOX1) was purified after heterologous expression in *E. coli*. The recombinant protein was obtained with a purity of 95% and a yield of 50 μg per liter of *E. coli* culture. Site directed mutagenesis of the hAOX1 cDNA allowed purification of proteins variants bearing the amino acid exchanges R802C, R921H, N1135S and H1297R corresponding to some of the identified SNPs. The hAOX1 variants were purified and compared to the wild-type protein relative to activity, oligomerization state, and metal content. Our data show that mutation of each amino acid residue has a variable impact on hAOX1 ability to metabolize selected substrates. Thus the human population is characterized by the presence of functionally inactive hAOX1 allelic variants as well as variants coding for enzymes with different catalytic activity. Our results indicate that the presence of these allelic variants should be considered for the design of future drugs.

DMD Fast Forward. Published on January 25, 2012 as DOI: 10.1124/dmd.111.043828
This article has not been copyedited and formatted. The final version may differ from this version.

Introduction

Aldehyde oxidase (AO, EC1.2.3.1) is a molybdo-flavoenzyme present in the cytosolic compartment of many tissues in various animal species, including humans (Garattini*, et al.*, 2008, Garattini*, et al.*, 2009). AO is a member of the xanthine oxidase (XO) family, which consists of complex metallo-flavoproteins containing two [2Fe2S] clusters, FAD and the molybdenum cofactor (Moco) as the catalytically active units (Hille, 1996). The AO holoenzyme is a homodimer and each 150 kDa monomer is characterized by three separate domains: the 20 kDa N-terminal domain binds the two distinct [2Fe-2S] clusters, FeSI and FeSII, the 40 kDa central domain binds FAD and the 80 kDa C-terminal domain binds Moco (Garattini*, et al.*, 2003). Members of the XO family of molybdoenzymes are characterized by an equatorial sulfur ligand at the Moco, essential for enzyme activity (Edmondson*, et al.*, 1972, Wahl & Rajagopalan, 1982).

AO is found in most animal species including fish and insects (Garattini*, et al.*, 2008). In humans, AO is encoded for by a single functional gene, *hAOX1*. Although *hAOX1* orthologues are found in almost all mammalian organisms, the number of functional *AOX* genes varies according to the species considered. Rodents contain the largest number of *AOX* functional genes: *Aox1*, *Aox3*, *Aox4* and *Aox3l1 (Garattini, et al., 2009)*. These genes arose from a series of gene duplication events from a common ancestor and are clustered on a short region of mouse chromosome 1 and rat chromosome 9. All the products of the mammalian *AOX* genes have high amino acid sequence similarity and are expressed in a tissue-specific manner in different organisms (Garattini*, et al.*, 2003, Terao*, et al.*, 2006). It is believed that the various AOX isoforms recognize distinct substrates and carry out different physiological tasks. The tissue distribution of mouse mAOX3 is superimposable to that of mAOX1, and the two enzymes are predominantly synthesized in liver, lung, and testis (Vila*, et al.*, 2004). The expression of mAOX4 is limited to the harderian gland, oesophagus and skin, while mAOX3L1 expression is restricted to the nasal mucosa (Terao*, et al.*, 2000). Except for mAOX4, which metabolizes retinaldehyde into retinoic acid and plays a role in skin

homeostasis (Terao*, et al.*, 2009), very little is known about the specific substrates and the physiological role of mAOX1 or any of the other AOX homologues.

In spite of this lack of information on the physiological significance of the AO enzymes, hAOX1 has long been recognized as a prominent drug metabolizing enzyme (Obach*, et al.*, 2004, Pryde*, et al.*, 2010, Garattini & Terao, 2011). AOX1 is characterized by broad substrate specificity, catalyzing the oxidation of a wide range of endogenous and exogenous aldehydes as well as N-heterocyclic aromatic compounds (Kitamura*, et al.*, 2006). In addition, AOX1 catalyzes the reduction of a variety of functional groups including sulfoxides, N-oxides, azo dyes, and N-hydroxycarbamoyl substituents in the presence of an appropriate donor. N-heterocyclic drugs such as methotrexate, 6-mercaptopurine, cinchona alkaloids, and famciclovir are also oxidized by this enzyme (Obach*, et al.*, 2004, Kitamura*, et al.*, 2006). Finally, AOX1 is involved in the oxidation of intermediary drug metabolites, such as the conversion of cyclic iminium ions arising from the cytochrome P450-catalyzed oxidation of pyrrolidines and piperidines into lactams, or the oxidation of aldehydes deriving from alcohol-containing drugs (Beedham, 1997).

Marked species differences have been well documented for the aldehyde-catalyzed metabolism of drugs, including methotrexate and farmciclovir (Rashidi*, et al.*, 1997, Jordan*, et al.*, 1999, Kitamura*, et al.*, 1999). An inter-individual variability of hAOX1 in vitro activity has been reported in humans (Kitamura*, et al.*, 1999, Al-Salmy, 2001), although the underlying determinants of these variations have never been investigated (Beedham*, et al.*, 2003). Gender may be one such determinant. In fact, male mice exhibit a 2-4 fold higher AO activity than female mice (Beedham, 1985, Kurosaki*, et al.*, 1999, Al-Salmy, 2001). It has also been suggested that factors such as age, cigarette smoking, drug usage, and disease states, such as cancer, may also account for the inter-individual variability of hAOX1 activity (Pryde*, et al.*, 2010). One final and prominent source of inter-individual variation is represented by missense single nucleotide polymorphisms (SNPs) affecting the catalytic activity of the hAOX1 enzyme. Numerous SNPs of the *hAOX1* gene are available in the NCBI dbSNP database,

although for the majority of them data on the frequency in the human population are not available. In addition, no single human SNP has been characterized for its affect on the catalytic activity of the purified enzyme. The only available functional studies on AOX1 SNPs were reported in Donryu rats (Adachi*, et al.*, 2007, Itoh*, et al.*, 2007, Itoh*, et al.*, 2007, Itoh*, et al.*, 2007). The functional characterization of the identified SNPs permitted the classification of these rats into ultrarapid metabolizer, extensive metabolizers and poor metabolizers according to the AOX1 mutation considered.

Inter-individual differences in hAOX1 activity are of primary importance for the clinical use of drugs known to be metabolized by the enzyme. They are also very important factors to be considered in the development of new drugs. For these reasons we decided to focus on this aspect of hAOX1 biology. Here, we report on the identification of relatively frequent hAOX1 SNPs and define their frequency in the Italian population. The most frequent missense SNPs were selected to produce the corresponding recombinant hAOX1 variant proteins, using an efficient *E. coli* expression system. The enzymatic and kinetic characteristics of the canonical hAOX1 and the variant proteins were compared. Our data provide evidence for the existence of frequent hAOX1 allelic variants defining fast and poor metabolizers in the human population.

Materials and Methods

Identification of SNPs

Blood samples (3 ml) were collected from 180 (67 males and 113 females) volunteers with following signing of a written consens. Thirty of these individuals were healthy volunteers, while the remaining 150 were individuals recruited for an unrelated epidemiological study. All samples were treated anonymously according to the guidelines of the internal Ethical Committee of the Istituto “Mario Negri”. The genomic DNA was extracted from blood samples by semi-automated vacuum-based nucleic acids extractor (AB6100, Applied Biosystems). Oligonucleotides were synthesized by Invitrogen (San Giuliano Milanese, MI, Italy). The genomic DNA fragments containing each the exon sequences were amplified using the oligonucleotides listed in supplementary files (Supplement Table I), using the Taq DNA polymerase kit (Applied Biosystems, Carlsbad, CA). The amplified PCR products (30-60ng) were sequenced in 96-well plates by Primm srl (Milano, Italy).

Cloning, Expression and Purification of human AOX1 and variants

Cloning of hAOX1 cDNA into pQE-30 Xa vector and PCR mutagenesis of the variants R921H and N1135S were done after Alfaro *et al.* (Alfaro*, et al.*, 2009). For site-directed mutagenesis of hAOX1 R802C and H1297R variants, the expression vector pQE-30 Xa including hAOX1 cDNA were used as a template, resulting in plasmids pTHAO1 and pTHAO2. All used constructs express hAOX1 as a N-terminal fusion protein with a His_6-tag.

For expression in *E. coli*, the constructs were transformed into TP1000 (Δ*mobAB*) cells (Palmer*, et al.*, 1996). *E. coli* was grown at 30°C in LB medium supplemented with 150 µg/ml ampicillin, 1 mM molybdate and 20 µM IPTG. Cells were harvested by centrifugation after 24 h of growth and resuspended in 50 mM sodium phosphate buffer, pH 8.0, containing 300 mM NaCl and frozen at -20°C until purification.

Cells were lysed two times in a Cell Disruptor-System at 1.35 kbar (Constant Systems, Northhampton, UK). Cell fragments were removed by centrifugation and the

supernatant was mixed with 4 ml of Ni-nitriloacetic acid (NTA) resin (Qiagen, Hilden, Germany) per 14 L of cell growth and incubated for 20 min at low stirring speed. The mixture was transferred to a column and washed with 10 column volumes both of 50 mM sodium phosphate, 300 mM NaCl, pH 8.0 containing 10 mM imidazole and the same buffer containing 20 mM imidazole. Proteins were eluted from the resin with 50 mM sodium phosphate, 300 mM NaCl, pH 8.0 containing 250 mM imidazole. The buffer of the eluted proteins was changed to 50 mM Tris, pH 7.5, by using PD10 columns. For stabilization of the protein, 2.5 mM DTT was added to the buffer. For further purification, hAOX1 was loaded on a MonoQ 5/50 GL column (GE Healthcare, Munich, Germany) equilibrated in 50 mM Tris, pH 7.5, containing 1 mM EDTA and eluted with a linear gradient of the same buffer containing 1 M NaCl. Fractions were analyzed by SDS-PAGE and the ones containing hAOX1 were combined. hAOX1 was further purified on a Superdex 200 column (GE Healthcare, Munich, Germany), equilibrated in 50 mM TrisHCl, pH 7.5, containing 200 mM NaCl and 1 mM EDTA. Only the fractions containing the dimeric form of hAOX1 were combined and used for the kinetic studies.

SDS-polyacrylamide Gel Electrophoresis (PAGE)

SDS-PAGE was performed using 12% polyacrylamide gels described by Laemmli (Laemmli, 1970). Staining of the proteins were done by using Coomassie Blue R.

Enzyme assays

Steady state enzyme kinetics were performed with purified hAOX1in 50 mM Tris buffer, pH 7.5, containing 200 mM NaCl and 1 mM EDTA at 25°C in a final volume of 500 µL. The substrates benzaldehyde, phthalazine and chloroquinazolinone, were used in a range of 0.1-100 µM using dichlorphenolindophenol (100 µM) as electron acceptor. For phenanthridine, molecular oxygen was used as electron acceptor and the product phenanthridone was detected at 450 nm. Total enzyme concentration varied between 200-600 nM. Reactions monitored over a range of 60 seconds. Activities were calculated using the extinction coefficient of 16,100 $M^{-1}cm^{-1}$ at 600 nm for DCPIP and

4,775 $M^{-1}cm^{-1}$ at 450 nm for phenanthridone. Obtained data from three individual measurements were fitted non-linear using the equation of Michaelis-Menten to obtain the kinetic constants K_M and turnover numbers.

Metal and MPT Analysis

The molybdenum and iron content of purified hAOX1 was determined by induced coupled plasma optical emission spectroscopy (ICP-OES) on a Perkin-Elmer Optima 2100 DV. 500 µL protein samples with a final concentration of 5 – 10 µM were wet-ashed in the same volume of 65% nitric acid by incubation at 100°C for 24 hours. The samples were diluted with 4 ml of water. The multi-element standard solution XVI (Merck) was used as a reference. The resulting mass concentrations were calculated as a percent of protein saturation of both molybdenum and two [2Fe2S] in relation to a theoretical 100% saturation. MPT was converted to its fluorescent derivative Form A by adjusting the pH of the supernatant to 2.5 with HCl and heating at 95 °C for 30 min in the presence of iodine (Johnson*, et al.*, 1984). Excess iodine was removed by the addition of 55 µL of 1% w/v ascorbic acid, and the sample was adjusted with 1 M Tris to pH 8.3. Form A was obtained from Form A-phospho by the addition of 40 mM $MgCl_2$ and 1 unit of calf intestine alkaline phosphatase. Form A was isolated with 10 mM acetic acid on a QAE ion exchange column (Sigma), which was equilibrated in H_2O. Form A was identified and quantified by HPLC analysis with a C18 reversed phase HPLC column (4.6 × 250-mm ODS Hypersil; particle size 5 µm) with 5 mM ammonium acetate, 15% v/v methanol at an isocratic flow rate of 1 mL/min. In-line fluorescence was monitored by an Agilent 1100 series detector with an excitation at 383 nm and emission at 450 nm.

EPR Spectroscopy

Continuous wave electron paramagnetic resonance spectra at 9.4 GHz X-band were recorded on a home-built spectrometer (microwave bridge ER041MR from Bruker

Biospin, Newark, DE, lock-in amplifier SR810 from Stanford Research, Stanford, CA, microwave counter 53181A from Agilent, Santa Clara, CA) equipped with a Bruker SHQ resonator. An Oxford ESR 910 helium flow cryostat with an Oxford ITC503 temperature controller, Oxfordshire, UK, was used for temperature control. The magnetic field was calibrated using a Li/LiF standard with a known g-value of 2.002293±0.000002. hAOX1 samples with concentrations of 50 µM were reduced with 20-fold excess of dithionite anaerobically on an argon flow prepared in quartz tubes with 4 mm outer diameter. Reduction was achieved by adding a small volume of an anaerobic dithionite solution in order to generate the reduced Fe(II)/Fe(III) in the FeS clusters. Samples tubes were rapidly frozen in deep-cold ethanol after a color change confirmed successful reduction.

DMD Fast Forward. Published on January 25, 2012 as DOI: 10.1124/dmd.111.043828
This article has not been copyedited and formatted. The final version may differ from this version.

Results

Single nucleotide polymorphisms of the human AOX1 gene.

The *hAOX1* gene is characterized by a very complex structure consisting of 35 coding exons (Garattini*, et al.*, 2008). To identify relatively frequent SNPs in the coding region of the gene, we amplified by PCR and sequenced each *hAOX1* exon from genomic DNA belonging to a cohort of 180 volunteers, representative of the Italian population. The couple of exon-specific oligonucleotides used for the amplification corresponded to sequences upstream and downstream of each exon in intronic regions are shown in Suppl. Table I. The presence of *bona-fide* SNPs was verified by sequencing in both directions. In this population, we identified one non-sense mutation, five non-synonymous and one synonymous SNP (Table I). The non-sense mutation was located in exon 5 and is predicted to result in a very short and non-functional protein of 126 amino acids. This mutation was relatively frequent and caused haplo-insufficiency in 8 individuals. The most frequent missense mutation was an A-G transition resulting in the substitution H/R at position 1297. The SNP was localized in exon 34 and it was observed in 13 individuals, 6 of which were homozygous for the trait. Exon 34 appeared to be a mutational hotspot, as another relatively frequent SNP (C/T) resulting in the substitution S/L at position 1271, and a synonymous SNP were located in this exon. All the individuals carrying the S1271L SNP were heterozygous for the trait. A relatively frequent missense SNP corresponding to an A-G transition, causing the substitution N/S at position 1135, was identified in exon 30. Two further and rare non-synonymous SNPs were identified in exons 22 and 25. They were the result of a C-T (*R802C*) and G-A (*R921H*) transition, respectively.

Expression and purification of hAOX1.

A pre-requisite for the functional characterization of the identified SNPs was optimization of the system used for the purification of a catalytically active hAOX1 protein (Alfaro*, et al.*, 2009). To this purpose, recombinant hAOX1 was expressed as an N-terminal His_6-tag fusion protein in *E. coli* TP1000 using the protocol described for

DMD Fast Forward. Published on January 25, 2012 as DOI: 10.1124/dmd.111.043828
This article has not been copyedited and formatted. The final version may differ from this version.

mAOX1 (Schumann*, et al.*, 2009) with slight modifications. The protein was purified using Ni-NTA, anion-exchange and size-exclusion chromatography. We isolated a 95% pure protein (Figure 1) with a yield of 50 µg per liter of cell growth. After size-exclusion chromatography two major peaks were detected corresponding to calculated molecular masses of 300 kDa and 150 kDa, which represented the dimeric and monomeric forms of hAOX1 (Figure 1). The ratio between dimer and monomer was calculated to be 1.5:1. The formation of protein aggregates was also observed, however, aggregation was prevented by addition of 2.5 mM dithiothreitol during the purification (data not shown). Analysis of the purified hAOX1 protein on 12% SDS polyacrylamide gels revealed a dominant protein band corresponding to the calculated molecular mass of 150 kDa for hAOX1 (Figure 1). Three other less intense bands of lower molecular weight were visible in all SDS polyacrylamide gels. The three bands were analyzed by MALDI peptide mapping and identified to be degradation products of hAOX1. Similar bands were also observed in purified mouse mAOX3 (Mahro*, et al.*, 2011) and AOX1 protein preparations of murine and rat origin (Kundu*, et al.*, 2007, Schumann*, et al.*, 2009). These products were never detectable upon native PAGE (Kundu*, et al.*, 2007, Mahro*, et al.*, 2011) and fast protein liquid chromatography (FPLC). All this suggested that the observed degradation products are generated by the reductive conditions intrinsic to SDS-PAGE.

The UV-vis spectra of hAOX1 in its oxidized form displayed the typical features of MFE's (Figure 1). The A280/A450 ratio of 5.0 for the recombinant protein indicated high purity of the enzyme. The 450/550 absorbance ratio in the UV-vis spectrum was calculated to be 3.0 for the recombinant enzyme, demonstrating full saturation with FAD. Additionally, the FAD content of hAOX1 was determined to be 100% by quantification of the AMP content of the protein (data not shown).

Protein expression over an extended time at low temperature allows *E. coli* cells to produce sufficient amounts of Mo-MPT for an almost complete saturation of the enzyme with this cofactor (Leimkühler*, et al.*, 2004). The main problem of the recombinant system is represented by poor insertion of the terminal sulfido ligand

essential for enzyme activity. We determined a 60% saturation of recombinant hAOX1 with molybdenum and a 70% saturation of the 2x[2Fe2S] clusters with iron (Figure 2). The amount of active enzyme containing the Mo=S ligand was calculated from the reduction spectra. To this purpose, we compared the ratio of oxidized over benzaldehyde-reduced hAOX1 to the amount of enzyme reduced with in relation to the fully reduced enzyme with dithionite under anaerobic conditions (data not shown). This method showed a 30% saturation ratio of sulfurated Mo-MPT in hAOX1. Thus, only 50% of the Mo-MPT contained the terminal sulfur ligand. To increase the catalytically active fraction of hAOX1, we co-expressed the *hAOX1* and hMCSF (human Moco-sulfurase) cDNAs (Ichida*, et al.*, 2001). However, analysis of the purified hAOX1 showed no increase in the levels of sulfurated Mo-MPT (data not shown). A band corresponding to hMCSF was not detected in cell lysates after separation on SDS-PAGE, suggesting that the majority of hMCSF was expressed in inclusion bodies in an inactive form (data not shown). Thus, in all subsequent purification experiments, we decided to express only the *hAOX1* cDNA in TP1000 cells.

EPR spectroscopy of the hAOX1 [2Fe-2S] clusters.

The two [2Fe-2S] clusters were characterized by EPR spectroscopy. Figure 3 shows the EPR spectra of recombinant and dithionite-reduced wild-type hAOX1 along with the corresponding simulations. The spectra display signals from several superimposed paramagnetic species, which are usually observed in enzymes belonging to the XO family. However, the most prominent signals are the characteristic EPR signals assigned to the two iron sulfur centers FeSI and FeSII, which are similar for all members of the XO family that have been described to date (Hille, 1996, Parschat*, et al.*, 2001). FeSI has EPR properties showing a slightly rhombic g-tensor, similar to those of many other [2Fe-2S] proteins, being fully developed at relatively high temperatures (up to T = 80 K), while FeSII has unusual EPR properties for [2Fe-2S] species with a more rhombic g-tensor, showing lines with varying linewidths that can only clearly be observed at much lower temperatures (T < 30 K). The g-values and line

widths were evaluated by simulating the spectra using the *EasySpin* toolbox for Matlab (Stoll & Schweiger, 2006). In both proteins, FeSI has similar EPR properties, including the typical, rhombic g-tensor as observed for other [2Fe2S] of the ferredoxin-type (see Table 2). Under the experimental conditions used to reduce the proteins, no clear signals of the reduced flavin semiquinone (FAD) or Moco (Mo^{V}) were observed. The linewidths and positions of the FeS signals at lower temperatures were affected by magnetic interactions. The obtained g-tensor and line width for FeSI and FeSII of hAOX1 are almost identical to the values previously published for mAOX1 (Schumann*, et al.*, 2009) or mAOX3 indicating high structural similarity among the proteins as expected from the amino acid sequence identity of 83% and 61%, respectively.

Purification and characterization of the hAOX1 polymorphic variants.

We studied the four most frequent hAOX1 SNPs, R802C, R921H, N1135S, H1297R as to their influence on enzyme activity protein dimerization and cofactor insertion. AOs belong to the XO family of molybdoenzymes and are characterized by high amino acid identity to the oxidase (XO) and dehydrogenase (XDH) forms of xanthine oxidoreductase (Garattini*, et al.*, 2008). Given a 50% identity between the two proteins, we modeled the structure of hAOX1 against the crystal structure of XDH from *Bos taurus* (BtXDH, PDB code: 1FO4) to define the spatial localization of the amino acid residues modified by the SNPs (Figure 4). The hAOX1 model indicates that R802 and R921 lay in proximity of the Moco and the FeSI sites, N1135 is localized close to the dimerization domain, while H1297 maps to the surface of the protein.

All hAOX1 variants were expressed and purified under similar conditions as the wild-type protein. Differences of the oligomerization state of the variants and wild-type hAOX1 were identified by size exclusion chromatography. All variants showed an altered dimer/monomer ratio. In the case of the R802C variant, only 40% of the protein was in its dimeric form (Figure 5). In contrast, all other hAOX1 variants showed a higher dimer/monomer ratio, indicating a higher proportion of the active protein. Mutation of each of the four amino acid residues did not affect insertion of the [2Fe-2S] clusters, as

DMD Fast Forward. Published on January 25, 2012 as DOI: 10.1124/dmd.111.043828
This article has not been copyedited and formatted. The final version may differ from this version.

the iron content was similar to that of wild-type hAOX1. In fact, similar to wild-type hAOX1, all variants showed 70% saturation with iron (Figure 2). In R802C molybdenum saturation was increased to 80%, which is slightly higher than the 70% saturation observed in the wild-type protein and all the other variants (Figure 2). The variant hAOX1 proteins were purified and showed a purity comparable to that of the wild-type counterpart. The UV-vis absorption spectra of the purified variants showed the same characteristic features of all molybdo-flavoenzymes (Figure 5).

Steady state kinetics of hAOX1 wild-type and variants.

To determine the impact of the SNPs on the enzymatic activity, steady state kinetics were performed on variants hAOX1-R802C, hAOX1-R921H, hAOX1-N1135S and hAOX1-H1297R. All generated variants were tested in their ability to catalyze the conversion of benzaldehyde, phthalazine, phenanthridine and chloroquinazolinone as substrates (Table 3). The wild-type hAOX1 showed activities with all tested substrates with a k_{cat} in a range of 5-12 min^{-1} with K_M values between 1 and 7 µM. The best substrate was phenanthridine with a k_{cat} of 12.2 min^{-1}.

For comparison, the dimeric portion of the hAOX1 variants was also subjected to steady state kinetic analyzes. The R802C variant showed the most comparable kinetic data to the wild-type protein. For the hAOX1-N1135S and hAOX1-H1297R variants the turnover numbers were increased 2.5-fold with phenanthridine as substrate. With other substrates the k_{cat} and K_M values remained in the same range of the wild-type protein for the two variants. The hAOX1-R921H variant showed a 3.7-1.5-fold decrease in k_{cat} with most of the substrates in comparison to the wild-type protein, while the K_M remained the comparable. Only with phenanthridine as substrate, the protein was completely inactive. The results show that the amino acid substitution has different influences on the kinetic constants depending on the substrate. The inactivity or reduced activity of the R921H variant might be explained by the fact that the arginine is highly conserved in all members of the XO family, and with its close proximity to the pterin molecule of the Mo-MPT cofactor, it might influence the geometry of the bound

Mo-MPT molecule, thus affecting catalytic turnover, while not affecting the binding of the substrate. However, since the different mutations affected the dimer/monomer ratio of the protein variants, we also considered the total amount of hAOX1 expressed and calculated the turnover number, taking into account the inactive portion of the monomeric protein. The normalized values are shown in Table 3. In general, the results show the same trends as the active portion of the protein.

Discussion

In this report we analyzed the impact of SNPs identified in hAOX1 in an Italian population. From a cohort of 180 healthy volunteers, representative of the Italian population, 7 different SNPs were identified which occurred with different frequencies. In total, 8 individuals were heterozygous for the exchange of Tyr126 to a stop codon. Another 8 individuals were heterozygous for a silent mutation in Leu1268. The most frequent mutations resulted in exchanges S1271L, which was identified in 14 individuals heterozygous for this mutation, and amino acid exchange H1297R, for which 7 individuals were heterozygous and 6 individuals were homozygous. Another mutation resulted in amino acid exchange N1135S, which was not so frequent and was identified in 1 individual heterozygous for this mutation and 4 individuals homozygous for this mutation. Two other rather rare mutations resulted in amino acid exchanges R802C and R921H, for which 2 and 1 individual, respectively, were heterozygous. We decided to characterize the mutations resulting in AOX1-variants H1297R, N1135S, R802C and R921H further, since they seemed to be the most interesting SNPs, because either they were rather frequent and might have an impact on human metabolism, or additionally homozygous individuals were identified. However, for the characterization of the hAOX1 variants, first a detailed characterization of the wild-type protein was required. A heterologous expression system for hAOX1 had been described before (Alfaro*, et al.*, 2009), however, here the protein was only partially purified and characterized only in terms of its activity with 6-substituted quinazolinones. In this report, we optimized the expression and purification of hAOX1 from *E. coli*. The protein was purified to almost

homogeneity, with minor degradation products, which became visible after SDS-PAGE. Characterization of the active portion of the protein showed that it was purified in a form with a molybdenum saturation of 70%, of which 50% contained the terminal sulfido ligand essential for activity. Thus, hAOX1 was purified in a form of which 30% was active. This is consistent with other reports of the purification of AOX1 and AOX3 from mouse (Schumann*, et al.*, 2009, Mahro*, et al.*, 2011) or of XDH purified from a baculovirus insect cell system (Nishino*, et al.*, 2002). Thus, apparently when using heterologous expression systems, the terminal sulfido ligand seems to be the limiting step to obtain a fully active mammalian enzyme. The iron saturation was determined to be 70%. The EPR spectra of hAOX1 were found to be very similar to those from the mAOX1 protein, showing a slightly rhombic signal for FeSI while FeSII has unusual EPR properties for [2Fe-2S] species with a pronounced rhombic g tensor, showing broad lines and being only observed at much lower temperatures (20 K). Overall, the close similarity of the EPR parameters indicated the presence of the same ligands and similar geometries of the two redox centers in comparison to mAOX1, which was expected from the high amino acid sequence identity of the two enzymes of 83%. While expression of AOs from mouse shows moderate protein yield (Schumann*, et al.*, 2009, Mahro*, et al.*, 2011), only low yield was achieved for the human AOX1 protein, suggesting major influences due to the difference in codon usage between *H. sapiens* and *E. coli*. A codon optimized construct for expression in *E. coli* will be tested in future studies to increase the protein yield.

Our characterization of the hAOX1 wild-type allowed us to have a good basis for the characterization of the SNPs. First, modelling of the amino acid exchanges in the *bovine* XDH gave us an idea of their locations in the protein. The crystal structure of eukaryotic AO is not available so far, however, attempts to solve the structure of the human and mouse proteins are in progress (unpublished data). The amino acid exchanges resulting from the SNPs were introduced into the protein and the respective variants were stable and showed an overall molybdenum and iron content similar to the wild-type protein, with the exception of the hAOX1-R802C variant which showed a

slightly higher saturation of Moco. The UV-vis spectra were also comparable to hAOX1 wild-type, suggesting a completely saturation of the FAD cofactor. However, in contrast to the overall cofactor composition, crucial changes were observed in the protein quaternary structures. While the wild-type enzyme is stable in its monomeric and dimeric form in a ratio of 1:1.5, the hAOX1-R921H, hAOX1-N1125S and hAOX1-H1297R variants were mainly purified as a stable dimer. In contrast, the hAOX1-R802C variant showed much higher levels of monomer in solution in a ratio of 1.5:1, resulting in a higher proportion of inactive protein. A change in monomer/dimer ratio has been reported before for similar variants in AO and XDH enzymes lying in proximity to the FeS clusters. In SNPs identified in Donryu rat strains the amino acid exchange G101S in proximity to FeSII also resulted in the production of the monomeric form of AOX1 (Itoh*, et al.*, 2007). In addition, in a human patient suffering from xanthinuria I, a mutation was identified in the *XDH* gene resulting in the amino acid exchange R149C (Sakamoto*, et al.*, 2001). The arginine is located in close proximity to FeSI and when this mutation was introduced in the *Rhodobacter capsulatus xdhB* gene and the corresponding RcXDH-R135C variant was characterized, the purified protein also existed in two forms, a monomeric inactive form and a dimeric active form (Leimkühler*, et al.*, 2003). Further analyses of the monomer/dimer behavior of *R. capsulatus* XDH resulted in a model in which it was proposed that dimerization of the two requires that the two FeS clusters are assembled correctly before Moco can be inserted and the protein can dimerize via the Moco domain (Schumann*, et al.*, 2008). Thus, amino acid exchanges in proximity to the FeS clusters influence the structure of the protein in a manner that dimerization is no longer effective.

We studied the activities of hAOX1 wild-type in comparison to the selected variants based of the SNPs with four selected substrates, benzaldehyde, phthalazine, phenanthridine and chloroquinazolinone. Our results show that the SNPs can be classified into three groups in general: fast metabolizers (FM), poor metabolizers (PM) and no affect on catalytic efficiency. Taking into account only the active portion of the protein, the hAOX1-R802C variant and even more pronounced the hAOX1-R921H

variant are PM, since both variants had a 2.4-1.5-fold reduced activity with most of the substrates tested. In addition, the R921H variant was identified to be inactive with phenanthridine, thus, the influence of the amino acid substitution on enzyme activity varies depending on the substrate. The hAOX1-N1135S and hAOX1-H1297R variants can be classified into FM, since an increased catalytic efficiency of 2-4-fold was observed depending on the tested substrate (taking into account only the active portion of the protein). In general, for the catalytic efficiencies, we calculated the overall activity of the purified enzyme taking into account the active and the inactive portion of the protein. In general, the same trends of kinetic values were obtained for the variants in comparison to the wild-type protein. The hAOX1-R921H variant showed that this residue is important for maintaining the catalytic activity of hAOX1, in particular with phenanthridine as substrate. Residue Arg921 lies close to Moco and affected mainly the monomer/dimer ratio, but also the overall activity of the protein. This might suggest that not only substrate turnover and binding was impaired, but also the intra-molecular electron transfer. Thus the positive charge of the arginine might affect substrate binding and intra-molecular electron transfer, which can only poorly be substituted for by His. In contrast, in the hAOX1-R802C variant the catalytic efficiency of the protein was not affected and we obtained similar values in comparison to the hAOX1 wild-type. Both hAOX1-N1135S and hAOX1-H1297R are considered to be FM variants of hAOX1. Especially with phthalazine and phenanthridine a 2-4 fold higher catalytic efficiency was obtained. Both amino acids are located at the surface of the protein and seem to influence the stability of hAOX1. Thus the more polar and positive charged residues seem to affect the surface charge of the protein which results in a higher stability of hAOX1. This also might influence the interaction with other proteins and/or posttranslational modifications of the protein, as suggested by Itoh et al. (Itoh*, et al.*, 2007) in a report on the characterization of SNPs in Donryu rats.

Our studies reveal the importance to consider individual differences based on SNPs for drug design. We analyzed 180 healthy individuals representative of the Italian population, and identified the total occurrence of 51 SNPs in hAOX1, and a total of 10

were homozygous for the SNP. Two of the SNPs resulted in FM and one in PM individuals. hAOX1 is an important enzyme responsible for the metabolism of a number of drugs containing aldehydes, and the more prevalent nitrogen heterocycles (Kitamura*, et al.*, 2006, Torres*, et al.*, 2007). The fraction of drugs metabolized by hAOX1 is likely to increase over the next decade. Thus, it should be carefully considered which dose of the drug is administered to an individual, since our results indicate that there might be a difference in hAOX1 activity in different individuals containing SNPs which additionally varies depending on the substrate used, thus in FM the drug might be cleared too fast and have no affect while in PM the drug might reach a toxic dose which would cause more severe side effects. Additionally, some individuals were identified with SNPs that resulted in nonsense mutations, which might even affect the overall hAOX1 content and thus the overall activity more drastically when the active protein amount is expressed only from one allele. In the future, hAOX1 activities should be measured in individuals with known SNPs or a pharmacokinetic study with a hAOX1 cleared drug in genotyped individuals should be conducted to confirm our results on the purified enzyme variants.

Acknowledgements:

We thank Manfred Nimtz (Braunschweig) for MALDI peptide mapping. We are grateful to T. Nishino and T. Matsumura (Nippon Medical School, Tokyo) for providing human Moco sulfurase cDNA.

Authorship Contributions.

Participated in research design: Hartmann, Terao, Garattini, Teutloff, Jones, Leimkühler

Conducted experiments: Hartmann, Terao, Teutloff, Alfaro

Performed data analysis: Hartmann, Terao, Garattini, Teutloff, Leimkühler

Wrote or contributed to the writing of the manuscript: Hartmann, Garattini, Jones, Leimkühler

REFERENCES

Adachi M, Itoh K, Masubuchi A, Watanabe N & Tanaka Y (2007) Construction and expression of mutant cDNAs responsible for genetic polymorphism in aldehyde oxidase in Donryu strain rats. *Journal of biochemistry and molecular biology* **40**: 1021-1027.

Al-Salmy HS (2001) Individual variation in hepatic aldehyde oxidase activity. *IUBMB life* **51**: 249-253.

Alfaro JF, Joswig-Jones CA, Ouyang W, Nichols J, Crouch GJ & Jones JP (2009) Purification and mechanism of human aldehyde oxidase expressed in Escherichia coli. *Drug metabolism and disposition: the biological fate of chemicals* **37**: 2393-2398.

Beedham C (1985) Molybdenum hydroxylases as drug-metabolizing enzymes. *Drug Metab. Rev.* **16**: 119-156.

Beedham C (1997) The role of non-P450 enzymes in drug oxidation. *Pharmacy world & science : PWS* **19**: 255-263.

Beedham C, Miceli JJ & Obach RS (2003) Ziprasidone metabolism, aldehyde oxidase, and clinical implications. *Journal of clinical psychopharmacology* **23**: 229-232.

Edmondson D, Massey V, Palmer G, Beacham LM, 3rd & Elion GB (1972) The resolution of active and inactive xanthine oxidase by affinity chromatography. *J Biol Chem* **247**: 1597-1604.

Garattini E & Terao M (2011) Increasing recognition of the importance of aldehyde oxidase in drug development and discovery. *Drug metabolism reviews* **43**: 374-386.

Garattini E, Fratelli M & Terao M (2008) Mammalian aldehyde oxidases: genetics, evolution and biochemistry. *Cell Mol Life Sci* **65**: 1019-1048.

Garattini E, Fratelli M & Terao M (2009) The mammalian aldehyde oxidase gene family. *Human genomics* **4**: 119-130.

Garattini E, Mendel R, Romao MJ, Wright R & Terao M (2003) Mammalian molybdo-flavoenzymes, an expanding family of proteins: structure, genetics, regulation, function and pathophysiology. *Biochem J* **372**: 15-32.

Hille R (1996) The mononuclear molybdenum enzymes. *Chemical Rev* **96**: 2757-2816.

Ichida K, Matsumura T, Sakuma R, Hosoya T & Nishino T (2001) Mutation of human molybdenum cofactor sulfurase gene is responsible for classical xanthinuria type II. *Biochem Biophys Res Commun* **282**: 1194-1200.

Itoh K, Maruyama H, Adachi M, Hoshino K, Watanabe N & Tanaka Y (2007) Lack of dimer formation ability in rat strains with low aldehyde oxidase activity. *Xenobiotica; the fate of foreign compounds in biological systems* **37**: 709-716.

Itoh K, Maruyama H, Adachi M, Hoshino K, Watanabe N & Tanaka Y (2007) Lack of formation of aldehyde oxidase dimer possibly due to 377G>A nucleotide substitution. *Drug metabolism and disposition: the biological fate of chemicals* **35**: 1860-1864.

Itoh K, Masubuchi A, Sasaki T*, et al.* (2007) Genetic polymorphism of aldehyde oxidase in Donryu rats. *Drug metabolism and disposition: the biological fate of chemicals* **35**: 734-739.

Johnson JL, Hainline BE, Rajagopalan KV & Arison BH (1984) The pterin component of the molybdenum cofactor. Structural characterization of two fluorescent derivatives. *J. Biol. Chem.* **259**: 5414-5422.

Jordan CG, Rashidi MR, Laljee H, Clarke SE, Brown JE & Beedham C (1999) Aldehyde oxidase-catalysed oxidation of methotrexate in the liver of guinea-pig, rabbit and man. *The Journal of pharmacy and pharmacology* **51**: 411-418.

Kitamura S, Sugihara K & Ohta S (2006) Drug-metabolizing ability of molybdenum hydroxylases. *Drug metabolism and pharmacokinetics* **21**: 83-98.

Kitamura S, Nakatani K, Sugihara K & Ohta S (1999) Strain differences of the ability to hydroxylate methotrexate in rats. *Comparative biochemistry and physiology. Part C, Pharmacology, toxicology & endocrinology* **122**: 331-336.

Kitamura S, Sugihara K, Nakatani K*, et al.* (1999) Variation of hepatic methotrexate 7-hydroxylase activity in animals and humans. *IUBMB life* **48**: 607-611.

Kundu TK, Hille R, Velayutham M & Zweier JL (2007) Characterization of superoxide production from aldehyde oxidase: an important source of oxidants in biological tissues. *Arch Biochem Biophys* **460**: 113-121.

Kurosaki M, Demontis S, Barzago MM, Garattini E & Terao M (1999) Molecular cloning of the cDNA coding for mouse aldehyde oxidase: tissue distribution and regulation in vivo by testosterone. Vol. 341 ed.^eds.), p.^pp. 71-80.

Laemmli UK (1970) Cleavage of structural proteins during the assembly of the head of bacteriophage T4. *Nature* **227**: 680-685.

Leimkühler S, Hodson R, George GN & Rajagopalan KV (2003) Recombinant *Rhodobacter capsulatus* xanthine dehydrogenase, a useful model system for the characterization of protein variants leading to xanthinuria I in humans. *J Biol Chem* **278**: 20802-20811.

Leimkühler S, Stockert AL, Igarashi K, Nishino T & Hille R (2004) The role of active site glutamate residues in catalysis of *Rhodobacter capsulatus* xanthine dehydrogenase. *J Biol Chem* **279**: 40437-40444.

Mahro M, Coelho C, Trincao J*, et al.* (2011) Characterization and Crystallization of Mouse Aldehyde Oxidase 3: From Mouse Liver to Escherichia coli Heterologous Protein Expression. *Drug metabolism and disposition: the biological fate of chemicals* **39**: 1939-1945.

Nishino T, Amaya Y, Kawamoto S, Kashima Y & Okamoto K (2002) Purification and characterization of multiple forms of rat liver xanthine oxidoreductase expressed in baculovirus-insect cell system. *Journal of biochemistry* **132**: 597-606.

Obach RS, Huynh P, Allen MC & Beedham C (2004) Human liver aldehyde oxidase: inhibition by 239 drugs. *Journal of clinical pharmacology* **44**: 7-19.

Palmer T, Santini C-L, Iobbi-Nivol C, Eaves DJ, Boxer DH & Giordano G (1996) Involvement of the *narJ* and *mob* gene products in the biosynthesis of the molybdoenzyme nitrate reductase in *Escherichia coli*. *Mol Microbiol* **20**: 875-884.

Parschat K, Canne C, Huttermann J, Kappl R & Fetzner S (2001) Xanthine dehydrogenase from Pseudomonas putida 86: specificity, oxidation-reduction potentials of its redox-active centers, and first EPR characterization. *Biochim Biophys Acta* **1544**: 151-165.

Pryde DC, Dalvie D, Hu Q, Jones P, Obach RS & Tran TD (2010) Aldehyde oxidase: an enzyme of emerging importance in drug discovery. *Journal of medicinal chemistry* **53**: 8441-8460.

Rashidi MR, Smith JA, Clarke SE & Beedham C (1997) In vitro oxidation of famciclovir and 6-deoxypenciclovir by aldehyde oxidase from human, guinea pig, rabbit, and rat liver. *Drug metabolism and disposition: the biological fate of chemicals* **25**: 805-813.

Sakamoto N, Yamamoto T, Moriwaki Y*, et al.* (2001) Identification of a new point mutation in the human xanthine dehydrogenase gene responsible for a case of classical type I xanthinuria. *Hum Genet* **108**: 279-283.

Schumann S, Saggu M, Möller N, Anker SD, Lendzian F, Hildebrandt P & Leimkühler S (2008) The mechanism of assembly and cofactor insertion into *Rhodobacter capsulatus* xanthine dehydrogenase. *J Biol Chem* **283**: 16602-16611.

Schumann S, Terao M, Garattini E, Saggu M, Lendzian F, Hildebrandt P & Leimkuhler S (2009) Site directed mutagenesis of amino acid residues at the active site of mouse aldehyde oxidase AOX1. *PloS one* **4**: e5348.

Stoll S & Schweiger A (2006) EasySpin, a comprehensive software package for spectral simulation and analysis in EPR. . *J Magn Reson* **178**: 42-55.

Terao M, Kurosaki M, Saltini G, Demontis S, Marini M, Salmona M & Garattini E (2000) Cloning of the cDNAs coding for two novel molybdo-flavoproteins showing high similarity with aldehyde oxidase and xanthine oxidoreductase. *J Biol Chem* **275**: 30690-30700.

Terao M, Kurosaki M, Barzago MM*, et al.* (2006) Avian and canine aldehyde oxidases. Novel insights into the biology and evolution of molybdo-flavoenzymes. *The Journal of biological chemistry* **281**: 19748-19761.

Terao M, Kurosaki M, Barzago MM*, et al.* (2009) Role of the molybdoflavoenzyme aldehyde oxidase homolog 2 in the biosynthesis of retinoic acid: generation and characterization of a knockout mouse. *Molecular and cellular biology* **29**: 357-377.

Torres RA, Korzekwa KR, McMasters DR, Fandozzi CM & Jones JP (2007) Use of density functional calculations to predict the regioselectivity of drugs and molecules metabolized by aldehyde oxidase. *Journal of medicinal chemistry* **50**: 4642-4647.

Vila R, Kurosaki M, Barzago MM*, et al.* (2004) Regulation and biochemistry of mouse molybdo-flavoenzymes. The DBA/2 mouse is selectively deficient in the expression of aldehyde oxidase homologues 1 and 2 and represents a unique source for the purification and characterization of aldehyde oxidase. *J Biol Chem* **279**: 8668-8683.

Wahl RC & Rajagopalan KV (1982) Evidence for the inorganic nature of the cyanolyzable sulfur of molybdenum hydroxylases. *J. Biol. Chem.* **257**: 1354-1359.

Footnotes:

This work was supported by the Cluster of Excellence ‘Unifying Concepts in Catalysis’ (C. Teutloff and S. Leimkühler) coordinated by the Technische Universität Berlin and funded by the Deutsche Forschungsgemeinschaft and by grants from the Associazione Italiana per la Ricerca contro il Cancro (AIRC) and the Fondazione Italo Monzino (E. Garattini).

Figure Legends:

Figure 1: Characterization of human aldehyde oxidase

Shown are the size-exclusion chromatogram of Superdex 200 purified hAOX1 and its UV-vis absorption spectrum. (A) Elution profile of a size-exclusion chromatography (Superdex 200) shows two peaks of hAOX1 wild-type protein corresponding to the dimeric (1) and monomeric (2) form in solution. The purity of the protein was determined by SDS-PAGE (D = dimer, M = monomer). Stars indicate degradation products of hAOX1 as determined by mass spectroscopy. (B) UV-vis spectrum of air oxidized hAOX1 in 50 mM Tris, pH 8.0 at 25°C showing characteristic absorptions of the protein bound FAD at 450 nm and a shoulder for the iron-sulfur clusters at 550 nm. The spectrum of the protein dimer is shown in black and the spectrum of the monomeric portion is shown in grey.

Figure 2: Saturation of hAOX1 with molybdenum and iron

Determination of the cofactor saturation of hAOX1 by ICP-OES. The iron content corresponds to saturation with both, FeSI and FeSII clusters. The wild-type protein and all variants show a similar saturation of 2x [2Fe2S], but vary in their molybdenum content between a saturation of 60% and 80% (D = dimer, M = monomer). The % values are related to theoretical full complement of Moco and the 2x[2Fe2S] clusters.

Figure 3: EPR spectra of hAOX1 wild-type.

Experimental cw-EPR spectra of dithionite-reduced mAOX1 wild-type samples at pH 7.0 (trace a) together with the corresponding simulation (trace b). For simulation parameters see Table 2. The flavin semiquinone and the (Mo^{V}) were not detected under these experimental conditions and therefore neglected in all simulations. (a) mAOX1 wild-type; (b) simulation of complete spectrum; (c) simulation of FeSI; (d) simulation of FeSII. Experimental conditions: T = 20 K, 1 mW microwave power,

microwave frequency 9.385 GHz, 0.5 mT modulation amplitude, 100 kHz modulation frequency.

Figure 4: Model of the locations of the amino acid exchanges as a result of SNPs identified in the *hAOX1* gene.

Model with program MacPyMOL using bovine XDH (pdb 1FO4). A = R793 (R802 in human AOX1), B = R912 (R921 in human AOX1), C = S1126 (N1135 in human AOX1), D = N1288 (H1297 in human AOX1). The amino acid which is affected by the SNPs is marked in red. The cofactors (Moco, FeS clusters and FAD) are shown in stick representations. The overall $(\alpha)_2$ structure is labeled in light grey for one subunit and in dark grey for the other subunit of the homodimer.

Figure 5: Size-exclusion-chromatography profiles and UV-vis-spectra of hAOX1 variants identified in SNPs.

Elution profiles of hAOX1 variants using size-exclusion chromatography on a Superdex 200 column and UV-vis-spectra of purified proteins are shown (A = R802C, B = R921H, C = N1135S, D = H1297R). In comparison to the wild-type protein, hAOX1 variants show different dimer/monomer ratios in solution. R802C is mainly purified in its monomeric form (A), whereas all other studied variants almost completely exist in their dimeric forms (B,C,D). For all variants, similar degradation products were visualized by SDS-PAGE as in the wild-type. (D = Dimer, M = Monomer, stars = degradation products of hAOX1, 1 = peak corresponding to the AOX1 dimer, 2 = peak corresponding to the AOX1 monomer)

DMD Fast Forward. Published on January 25, 2012 as DOI: 10.1124/dmd.111.043828
This article has not been copyedited and formatted. The final version may differ from this version.

Table 1: *Non-sense, missense and synonymous polymorphisms of the human AOX1 gene in the Italian population* The SNP data were deposited in the NCBI database under the accession numbers indicated in the last column.

Exon	Nucleotide	Amino acid	Allelic frequency	Heterozygotes	Homozygotes	RefSNP(rs)
5	C/G	Y126stop	0.026	8/153	0/153	ss469333481
22	C/T	R802C	0.006	2/180	0/180	rs41309768
25	G/A	R921H	0.003	1/180	0/180	rs56199635
30	A/G	N1135S	0.029	1/154	4/154	rs55754655
34	C/T	S1271L	0.039	14/178	0/178	rs141786030
34	A/G	H1297R	0.053	7/178	6/178	rs3731722
34	C/T	L1268silent	0.022	8/178	0/178	ss469333482

DMD Fast Forward. Published on January 25, 2012 as DOI: 10.1124/dmd.111.043828
This article has not been copyedited and formatted. The final version may differ from this version.

Table 2: EPR linewidths and g-values of FeSI and FeSII from hAOX1.

Protein	Cluster	g-values			Linewidth [mT][a]		
		g_x	g_y	g_z	ΔB_x	ΔB_y	ΔB_z
hAOX1	FeSI FeSII	2.0115 2.085	1.924 1.975	1.900 1.906	4.1 9.2	2.4 3.3	3.7 2.8
mAOX1[b]	FeSI FeSII	2.019 2.085	1.927 1.971	1.912 1.90	2.6 7.4	2.6 4.0	3.2 4.0

[a] The variable linewidth was included as g-strain in the simulations.

[b] Values for mAOX1 are taken from ref. (32).

DMD Fast Forward. Published on January 25, 2012 as DOI: 10.1124/dmd.111.043828
This article has not been copyedited and formatted. The final version may differ from this version.

Table 3: Steady-state kinetics of hAOX1 and variants corresponding to single nuclear polymorhpisms (SNPs)

Substrate			WT	R802C	R921H	N1135S	H1297R
Benzaldehyde	active portion	K_M [µM]	7.1 ± 0.6	7.6 ± 1.9	6.3 ± 1,2	6.7 ± 2.8	5.2 ± 1.8
		k_{cat} [min^{-1}]	6.4 ± 0.1	5.3 ± 0.3	1.7 ± 0,1	6.2 ± 0.3	6.4 ± 0.3
		k_{cat}/K_M [1/min*µM]	0.91 ± 0.17	0.70 ± 0.16	0.27 ± 0.08	0.92 ± 0.11	1.23 ± 0.17
	total protein	k_{cat} [min^{-1}]	2.7 ± 0.1	1.8 ± 0.3	1.1 ± 0,1	3.8 ± 0.3	2.6 ± 0.3
		k_{cat}/K_M [1/min*µM]	0.38 ± 0.17	0.24 ± 0.16	0.17 ± 0.08	0.57 ± 0.11	0.50 ± 0.17
Phthalazine	active portion	K_M [µM]	1.3 ± 0.3	0.9 ± 0.3	1.6 ± 0.3	1.2 ± 0,1	1.3 ± 0,2
		k_{cat} [min^{-1}]	5.6 ± 0.2	5.2 ± 0.3	2.4 ± 0.1	7.2 ± 0,1	5.4 ± 0.1
		kc_{at}/K_M [1/min*µM]	4.31 ± 0.67	5.78 ± 1.00	1.50 ± 0.33	6.00 ± 1.00	4.15 ± 0.50
	total protein	k_{cat} [min^{-1}]	2.3 ± 0.2	1.8 ± 0.3	1.5 ± 0.1	4,4 ± 0,1	2.9 ± 0.1
		k_{cat}/K_M [1/min*µM]	1.77 ± 0.67	2.00 ± 1.00	0.94 ± 0.33	3.67 ± 1.00	2.23 ± 0.50
Phenanthridine	active portion	K_M [µM]	3.9 ± 0.8	4.4 ± 0.4	n.d.	6.1 ± 1.0	4.1 ± 0.7
		k_{cat} [min^{-1}]	12.2 ± 0.5	10.2 ± 0.2	n.d.	32.6 ± 1.1	31.5 ± 1.0
		k_{cat}/K_M [1/min*µM]	3.13 ± 0.63	2.32 ± 0.50	-	5.34 ± 1.10	7.68 ± 1.43
	total protein	k_{cat} [min^{-1}]	5.3 ± 0.5	3.4 ± 0.2	n.d.	19.9 ± 1.1	16.9 ± 1.0
		k_{cat}/K_M [1/min*µM]	1.36 ± 0.63	0.77 ± 0.50	-	3.26 ± 1.10	4.12 ± 1.43
Chloroquinazolinone	active portion	K_M [µM]	5.2 ± 0.7	4.7 ± 0.7	4.5 ± 0.8	4.1 ± 0.5	5.8 ± 0.5
		k_{cat} [min^{-1}]	5.6 ± 0.1	5.4 ± 0.2	3.6 ± 0.1	6.5 ± 0.1	6.7 ± 0.2
		k_{cat}/K_M [1/min*µM]	1.08 ± 0.14	1.15 ± 0.29	0.80 ± 0.13	1.59 ± 0.20	1.16 ± 0.4
	total protein	k_{cat} [min^{-1}]	2.3 ± 0.1	1.8 ± 0.2	2.2 ± 0.1	4.0 ± 0.1	3.6 ± 0.2
		k_{cat}/K_M [1/min*µM]	0.44 ± 0.14	0.38 ± 0.29	0.49 ± 0.13	0.98 ± 0.20	0.62 ± 0.4
Oligomerization in solution	Dimer	percentage [%]	58	39	83	90	78
	Monomer	percentage [%]	38	58	13	7	17
	Multimer	percentage [%]	4	3	4	3	5

Benzaldehyde, phthalazine, phenanthridine and chloroquinazolinone were used as substrates to cover a range from aldehydes to N-heterocyclic compounds. Assays were performed photometrically using 2,6-dichlorphenol-indophenol as a final electron acceptor. With phenanthridine molecular oxygen was used as electron acceptor. n.d. indicates that no activity is detectable. Data are mean values from three independent measurements (+/- S.D.).

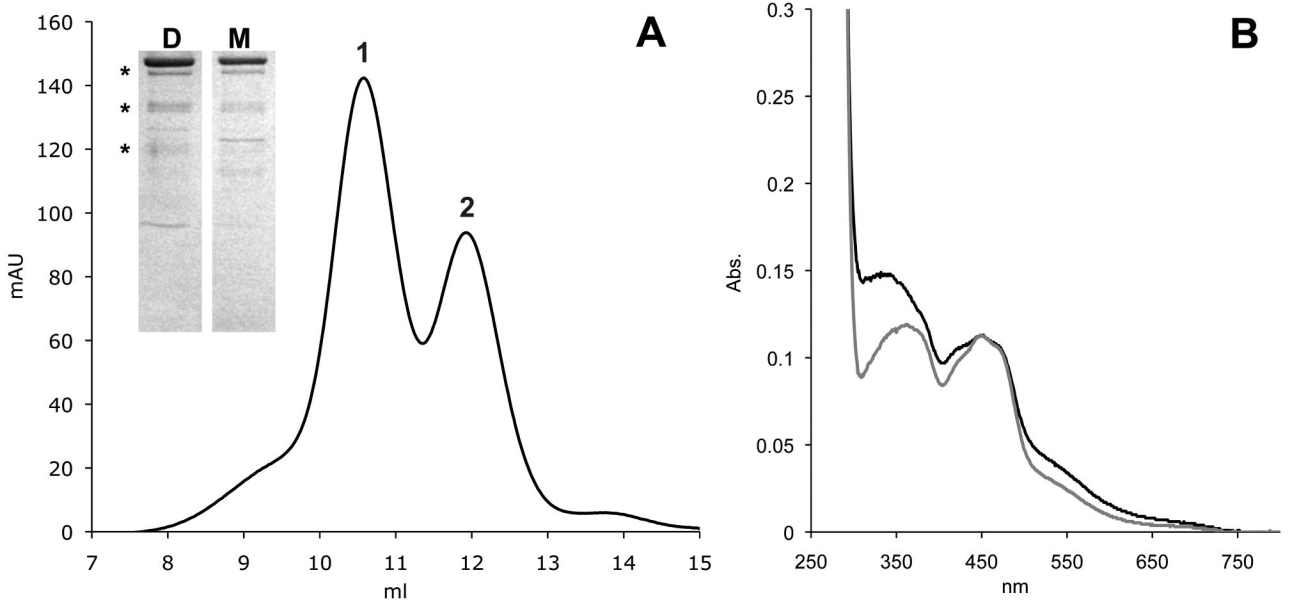
A
B
D
M
1
2
*
*
*
mAU
ml
Abs.
nm
160
140
120
100
80
60
40
20
0
7
8
9
10
11
12
13
14
15
0.3
0.25
0.2
0.15
0.1
0.05
0
250
350
450
550
650
750

Figure 1

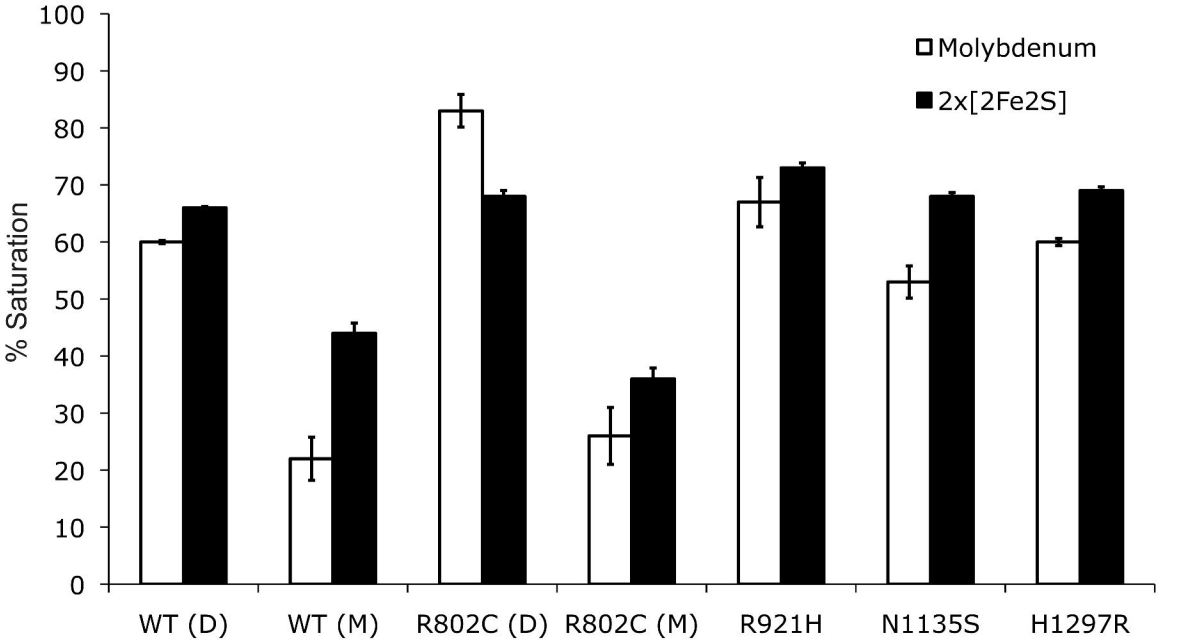
100
90
80
70
60
50
40
30
20
10
0
% Saturation
Molybdenum
2x[2Fe2S]
WT (D)
WT (M)
R802C (D)
R802C (M)
R921H
N1135S
H1297R

Figure 2

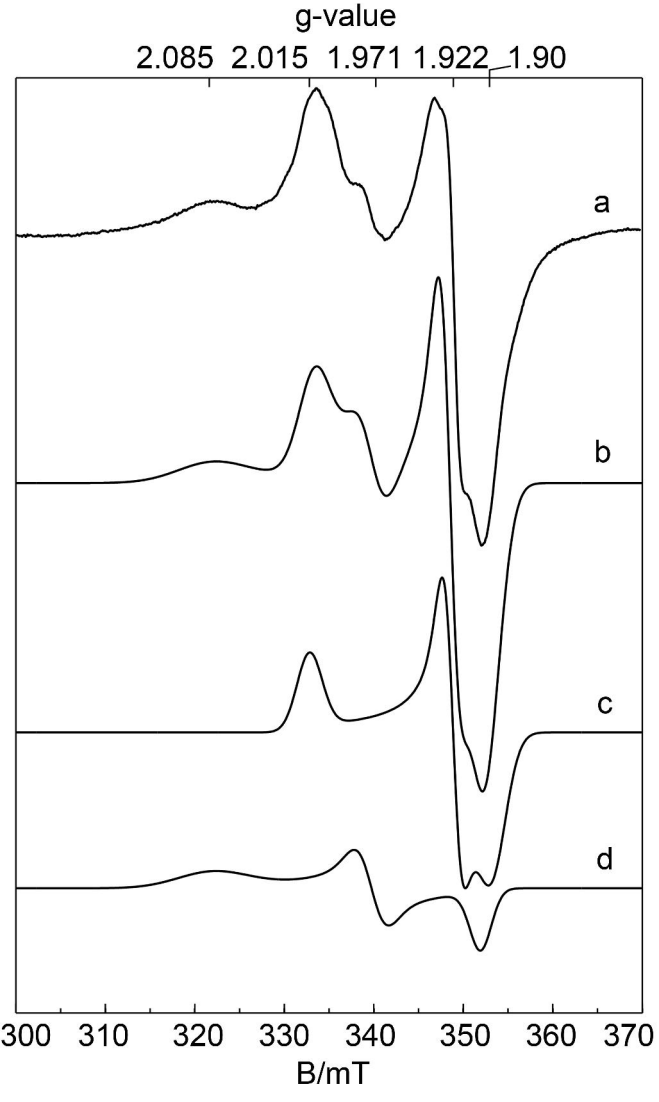
g-value
2.085
2.015
1.971
1.922
1.90
a
b
c
d
300
310
320
330
340
350
360
370
B/mT

Figure 3

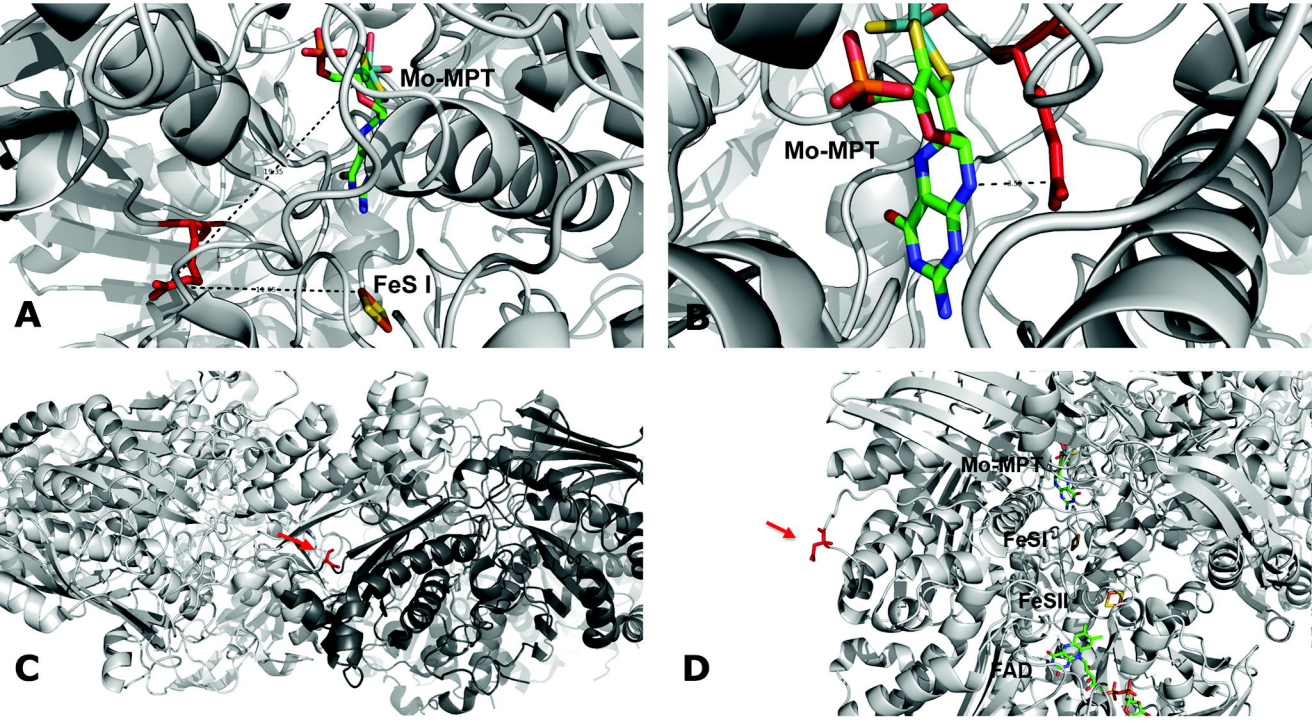

Figure 4

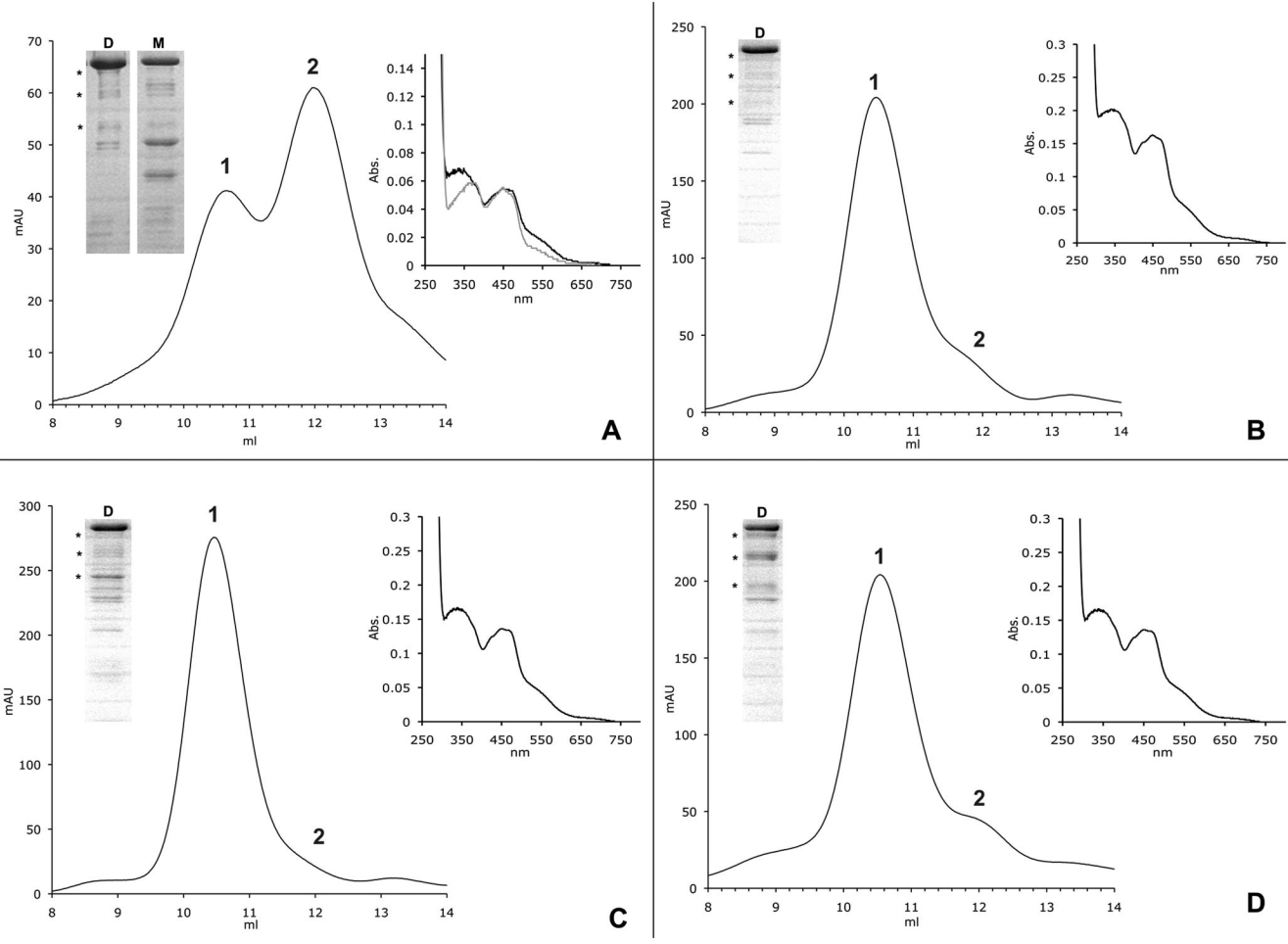

Figure 5